

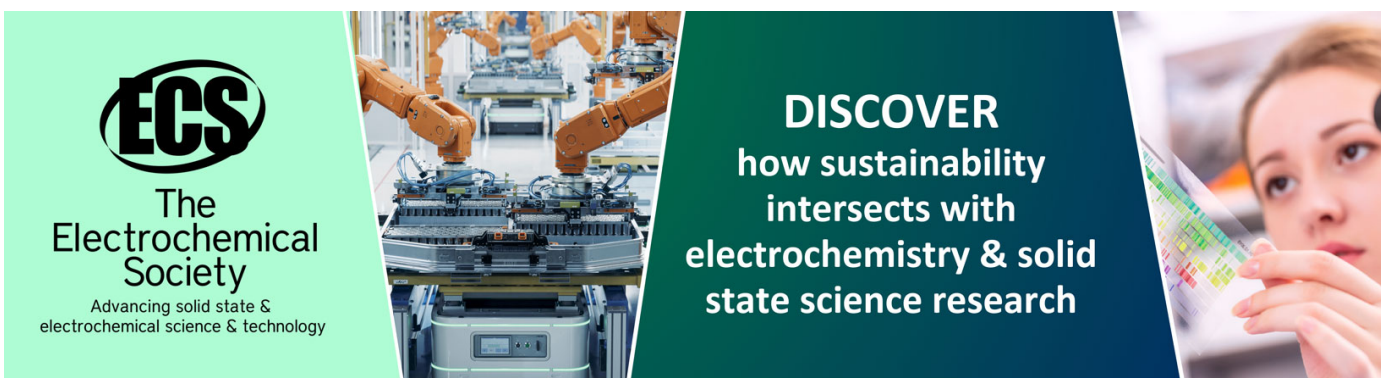
Preparation and characterization of hydroxyapatite/liposome core-shell nanocomposites

To cite this article: Maoquan Chu and Guojie Liu 2005 *Nanotechnology* **16** 1208

View the [article online](#) for updates and enhancements.

You may also like

- [Nanocomposite liposomes containing quantum dots and anticancer drugs for bioimaging and therapeutic delivery: a comparison of cationic, PEGylated and deformable liposomes](#)
Chih-Jen Wen, Calvin T Sung, Ibrahim A Aljuffali et al.
- [Liposome interaction with macrophages and foam cells for atherosclerosis treatment: effects of size, surface charge and lipid composition](#)
Jinkai Tang, Moumita Rakshit, Huei Min Chua et al.
- [Two cholesterol derivative-based PEGylated liposomes as drug delivery system. study on pharmacokinetics and drug delivery to retina](#)
Shengyong Geng, Bin Yang, Guowu Wang et al.



ECS
The
Electrochemical
Society
Advancing solid state &
electrochemical science & technology

DISCOVER
how sustainability
intersects with
electrochemistry & solid
state science research

Preparation and characterization of hydroxyapatite/liposome core–shell nanocomposites

Maoquan Chu^{1,3} and Guojie Liu²

¹ Institute of Life Science and Technology, Tongji University, Shanghai 200092, People's Republic of China

² Department of Chemistry, East China University of Science and Technology, Shanghai 200237, People's Republic of China

E-mail: mqchu98@yahoo.com.cn

Received 17 February 2005, in final form 12 April 2005

Published 20 May 2005

Online at stacks.iop.org/Nano/16/1208

Abstract

Hydroxyapatite (HAP)/liposome core–shell nanocomposites have been prepared at room temperature. The liposome shells and the precipitate cores ranged in diameter mainly from 80 to 140 nm and from 40 to 120 nm, respectively. Rod-like whiskers ranging in length mainly from 10 to 30 nm were obtained after separating the precipitates from the liposomes. In contrast, the whiskers synthesized without liposomes ranged in length mainly from 70 to 140 nm. The precipitates synthesized both with and without liposomes were poorly crystalline, and had a similar chemical composition to the natural HAP.

1. Introduction

Hydroxyapatite (HAP), $\text{Ca}_{10}(\text{PO}_4)_6(\text{OH})_2$, is the principle inorganic constituent of the hard tissues of animals. The HAP of bone is about $(1.5\text{--}3.5\text{ nm}) \times (5.0\text{--}10.0) \times (40.0\text{--}50.0)$ in size with a platelet shape [1]. Synthetic HAP has been mainly used clinically for artificial teeth and bones during the last three decades due to their biocompatibility, bioactivity, and osteoconduction characteristics with respect to the host tissues of animals [2]. The characteristics of the synthetic HAP, such as morphology, size, chemical composition and crystallinity, play important roles in biomedical applications.

However, even though HAP has the characteristics mentioned above, it has failed to become the nucleation sites for bone regeneration [3]. It is well known that lipid vesicles composed of bilayers of phospholipid molecules, so-called 'liposomes', have good biocompatibility due to the lipids being one of the major compositions of biological membranes. In order to improve the nucleation process for new bone formation, Hang *et al* [3] have used liposome-coated HAP and tricalcium phosphate as bone implants carried out in the mandibular bony defect of miniature swine, and they found that the liposome-coated materials were biocompatible and

their clinical endpoint was enhanced compared to those in the absence of liposomes. Moreover, they said that the liposomes had the ability to promote the repair of osseous deficiencies. Additionally, recent studies showed that HAP nanoparticles without sintering could inhibit DNA synthesis of W-256 sarcoma cells and lead to programmed cell death [4, 5] and inhibit proliferation, colony formation, depolymerization of microtubules and disruption of stress fibres in MGc-803 cells [6]. Liposome-coated HAP may be more easily internalized by endocytosis of tumour cells than bare HAP because the tumour cells have the capability of endocytic uptake of drug covered by a single lipid bilayer [7]. Preparation of HAP coated with liposomes with controlled morphology and size distribution, therefore, may be beneficial to therapy of bone disease and anticancer applications.

Though Feng *et al* [8] have used liposomes to synthesize HAP and calcium phosphate, their primary purpose was to study the biomineralization using liposomes as a model. In Feng's experiments, HAP solution (pH = 7) was encapsulated in phosphatidylcholine vesicles first, and then the precipitation formed within vesicles since the HAP solution was not stable and tends to deposit. However, they found that the product made from the precursor containing relatively high Ca^{2+} concentration (0.004 mol l^{-1}) could not be transformed into

³ Author to whom any correspondence should be addressed.

HAP unless it was soaked in hot water for 24 h. Unfortunately, both saturated and unsaturated phospholipids can be easily oxidized and hydrated to form lysophospholipids and fatty acids at high temperature [9, 10]; hot water is not suitable for the HAP synthesis if the liposome-coated HAP is to be used as a nanocomposite for biomedical implants and anticancer materials. Additionally, little work is present about liposome-coated HAP prepared from vesicles filled with a mixture solution of calcium nitrate tetrahydrate $[\text{Ca}(\text{NO}_3)_2 \cdot 4\text{H}_2\text{O}]$ and ammonium dibase phosphate $[(\text{NH}_4)_2\text{HPO}_4]$ in acidic conditions at low temperature.

To obtain HAP nanoparticles coated with lipid membrane, in this work, small unilamellar lipid vesicles encapsulating HAP have been prepared at room temperature. In our experiments, a mixture solution ($\text{pH} = 2.4$) of $\text{Ca}(\text{NO}_3)_2 \cdot 4\text{H}_2\text{O}$ and $(\text{NH}_4)_2\text{HPO}_4$ was first encapsulated within the intravesicular space; ammonia solution was then added to the extravesicular region after the removal of calcium ions outside liposomes by ion exchange. This technique had many advantages; for example, HAP could be formed directly within the liposomes without the temperature rise, and the oxidation and hydration of the lipid membrane would be reduced compared to that of the lipid treated at high temperature, etc. Additionally, more interesting findings were that (1) the products had obvious core-shell characteristics, (2) the HAP cores were composed of many rod-like nanoparticles, which had a similar crystallinity and chemical composition to the natural material, and (3) the liposomes not only acted as a constrained domain of size in the nanoscale for the purpose of intravesicular reaction and controlled the morphology and size distribution of the HAP nanoparticles, but also made the HAP cores stable and separated from each other. These core-shell nanocomposites may be of special interest for biomedical applications.

2. Experimental section

Soybean lecithin, $\text{Ca}(\text{NO}_3)_2 \cdot 4\text{H}_2\text{O}$, $(\text{NH}_4)_2\text{HPO}_4$, $\text{NH}_3 \cdot \text{H}_2\text{O}$, HNO_3 , and absolute ethanol were purchased from Shanghai Chemical Reagent Corporation. All the solvents and reactants except soybean lecithin were analytical grade. The soybean lecithin as well as the other reagents was used without further purification. Deionized water (Millipore 'milli-Q' unit) was used in all experiments.

For preparation of HAP/liposome core-shell nanocomposites, 500 mg soybean lecithin was dissolved in chloroform in a round bottomed flask and dried *via* rotary evaporation to make a thin film. The flask was placed in a vacuum desiccator overnight at room temperature to remove the last traces of chloroform. A 100 ml mixture of $\text{Ca}(\text{NO}_3)_2 \cdot 4\text{H}_2\text{O}$ and $(\text{NH}_4)_2\text{HPO}_4$, of which the pH value was adjusted to 2.4 with HNO_3 , was then used to hydrate the dry lipid film to form liposomes. The concentrations of $\text{Ca}(\text{NO}_3)_2 \cdot 4\text{H}_2\text{O}$ and $(\text{NH}_4)_2\text{HPO}_4$ were 0.25 and 0.15 mol l^{-1} , respectively. The vesicle suspension was emulsified by emulsiflex-B3 (Avestin, Canada) ten times. To obtain liposomes of uniform size, the solution was extruded through polycarbonate membrane filters (Poretics, USA) with a pore diameter of 200 nm. The extrusion was repeated 10 times. In order to remove the Ca^{2+} ions outside the vesicles, the suspension was passed through an

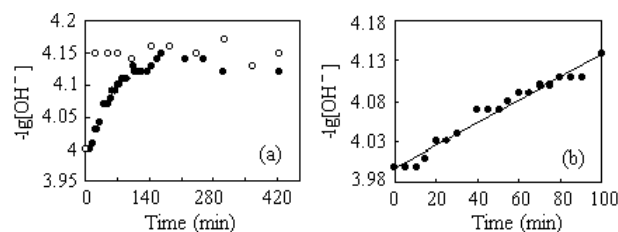


Figure 1. Plot of $-\lg[\text{OH}^-]$ versus time for HAP synthesized with (solid dots) and without (hollow dots) liposomes. The graph (b) is the relationship between $-\lg[\text{OH}^-]$ and time in the initial 100 min for HAP synthesized within liposomes.

ion exchange column of sodium form ($001 \times 7(732)$, Shanghai Chemical Reagent Corporation). $\text{NH}_3 \cdot \text{H}_2\text{O}$ solution was then added to the extravesicular region with continuous vigorous stirring at room temperature until the pH value reached 10.0. Additionally, HAP sol without liposomes was synthesized with $\text{Ca}(\text{NO}_3)_2 \cdot 4\text{H}_2\text{O}$ (0.25 mol l^{-1}) and $(\text{NH}_4)_2\text{HPO}_4$ (0.15 mol l^{-1}) at room temperature.

In order to evaluate the properties of the precipitates synthesized within liposomes, the samples were withdrawn at 2 h and 12 days after $\text{NH}_3 \cdot \text{HO}_2$ solution addition. The unstained samples of the liposomes encapsulating precipitations were air dried onto carbon coated grips and evaluated by transmission electron microscopy (TEM) using a JEOL JEM-200CX operating at 120 kV. For x-ray diffraction (XRD), Fourier-transform infrared (FT-IR) and x-ray photoelectron spectroscopy (XPS) evaluation, the samples were centrifuged and washed three times with 4% (v/v) triton X-100, absolute ethanol and deionized water, and then dried at 313 K for 48 h. XRD patterns were taken on a diffractometer (4654-2A1, LCCAS, Japan) using a Ni-filtered $\text{Cu K}\alpha$ ($\lambda = 0.15418$ nm) radiation. FT-IR spectra were characterized with an EQUINOX 55 spectrometer (Nicolet). The XPS pattern was performed on a NP-1 x-ray photoelectron spectroscope (Shengyang, China) with $\text{Mg K}\alpha$ radiation.

3. Results and discussion

In our experiments, no precipitates could be observed in a short time after adding $\text{NH}_3 \cdot \text{H}_2\text{O}$ solution to the vesicular suspension encapsulating ions; by contrast, a large amount of precipitate was observed rapidly in the similar precipitation reactions in the absence of liposomes. Slow precipitation within liposomes is due to slow permeation of hydroxide ions into intravesicular space. Figure 1 presents the rate of decrease of hydroxide ions in solution with time. We note that the concentration of hydroxide ions decreases rapidly in the case without liposomes, while for the synthesis within liposomes the concentration of hydroxide ions gradually decreases with time in the initial 100 min, and then retains the value of $10^{-4.14 \pm 0.02}$ mol l^{-1} . The first-order relationship between OH^- (hydroxide ions) and t (time) in the initial 100 min is obtained. The kinetic equation can be given by

$$\lg[\text{OH}^-] = -0.0014t - 3.9977$$

$$(R^2 = 0.9715) \quad (0 < t < 100 \text{ min}),$$

which implies that the HAP synthesis within liposomes is a diffusion-controlled mechanism.

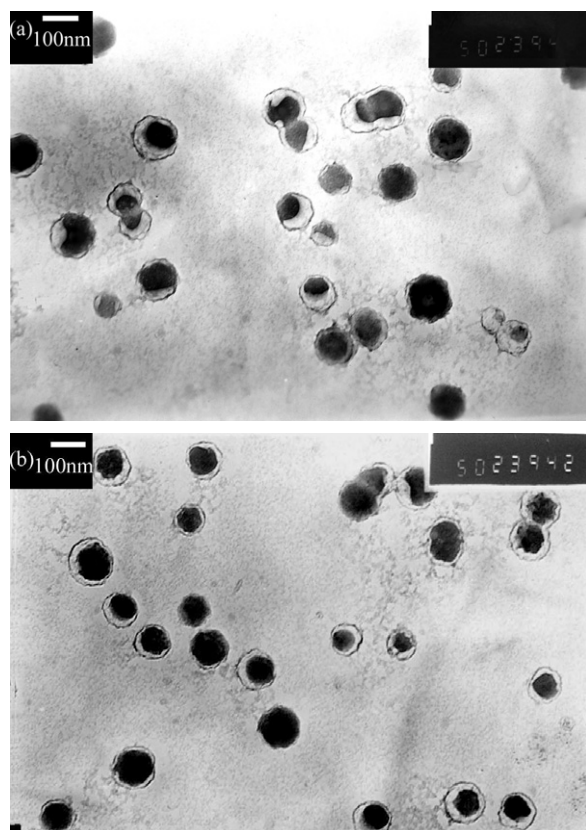


Figure 2. TEM images of liposome-coated precipitates withdrawn at (a) 2 h and (b) 12 days after $\text{NH}_3 \cdot \text{HO}_2$ solution addition.

Figure 2 shows the typical TEM images of the liposomes encapsulating precipitates. It is clear that most of the particles have spherical core-shell characteristics ranging in diameter mainly from 80 to 140 nm, and have almost no difference between the samples withdrawn at 2 h (figure 2(a)) and 12 days (figure 2(b)) after $\text{NH}_3 \cdot \text{HO}_2$ solution addition. The precipitates form only within the liposomes. The membranes of liposomes can be seen clearly in the case of being unstained by phosphotungstic acid, maybe due to the contrast created by adsorbed Ca^{2+} ions. Most of the core-shell composites locate separately even over 12 days, which indicates that the liposome shells are stable.

Though the intravesicular precipitates are nearly spherical shaped ranging in diameter mainly from 40–120 nm, they can be dispersed into rod-like nanoparticles after separating from the vesicles (figure 3(a)). The particles are separated from the samples as shown in figure 2(b) (because we find that the samples withdrawn at 2 h are similar to those withdrawn after 12 days in morphology, crystallinity, and chemical composition, only the samples withdrawn at 12 days are discussed as follows). We also note that the whiskers synthesized both with (figure 3(a)) and without (figure 3(b)) liposomes are of length ranging mainly from 10 to 30 nm and 70 to 140 nm, respectively, which indicates that the particle sizes are significantly reduced in the presence of liposomes. This result may be explained as follows: precipitates growing within liposomes is a heterogeneous nucleation process. As substrates of nucleation for nanoparticles formation, the

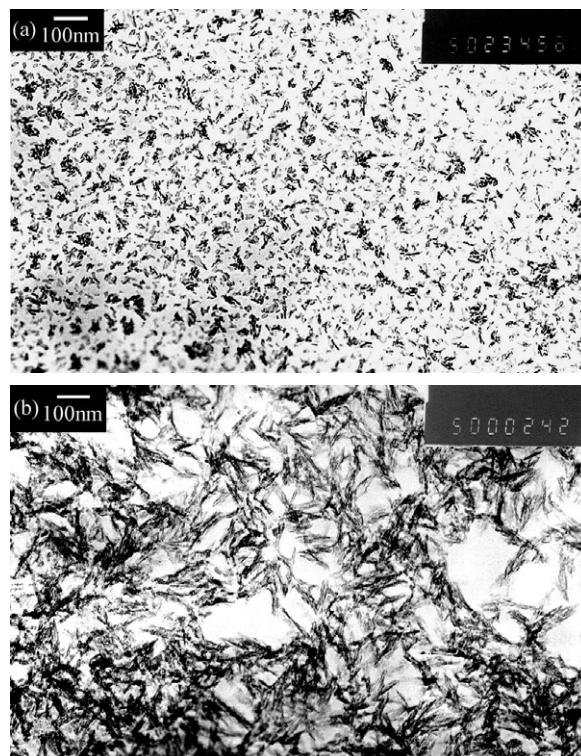


Figure 3. TEM images of precipitates (a) separated from liposomes and (b) synthesized in the absence of liposomes.

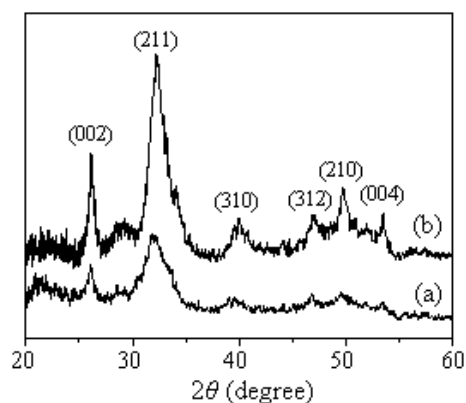


Figure 4. XRD spectra of precipitates (a) separated from liposomes and (b) synthesized in the absence of liposomes.

vesicular membranes can lower the activation energy of nucleation, so the nucleation rate of the precipitation within liposomes may be improved. However, the activation energy of crystal growth may increase due to the influx of hydroxide ions into liposomes being controlled by membranes; the growth rate of the precipitation within liposomes, therefore, may be lowered. Furthermore, the liposomes provide confined nanospace to prevent further growth of the whiskers. The sizes of whiskers synthesized within liposomes, therefore, are much smaller than those of whiskers outside liposomes.

The crystallinity of the precipitates is revealed by XRD patterns (figure 4). The precipitates synthesized both with and without liposomes have weak crystallized apatite phase and

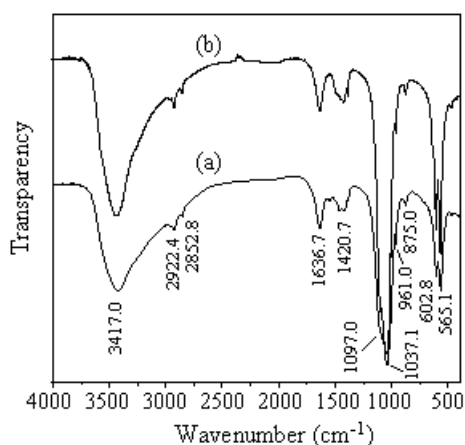


Figure 5. IR spectra of precipitates (a) separated from liposomes and (b) synthesized in the absence of liposomes.

Table 1. The d -spacings (Å) from diffraction peaks for precipitates grown with and without liposomes compared to those from the x-ray data card for HAP (No 1-1010) (intense peaks are underlined).

X-ray diffraction		X-ray data card (hexagonal HAP, No 1-1010)
Precipitate grown in the absence of liposomes	Precipitate grown within liposomes	
<u>3.41</u>	<u>3.43</u>	<u>3.44</u>
3.13	3.12	3.11
<u>2.77</u>	<u>2.81</u>	<u>2.79</u>
2.63	—	2.62
<u>2.25</u>	<u>2.27</u>	<u>2.27</u>
—	—	2.13
2.06	—	2.06
<u>1.93</u>	<u>1.94</u>	<u>1.94</u>
<u>1.83</u>	<u>1.84</u>	<u>1.84</u>
<u>1.71</u>	<u>1.71</u>	<u>1.71</u>

hardly contain any discernible crystalline impurity. A broad band ranging in 2θ from 30° to 35° is observed in both systems. We observe that the peaks of the spectrum in figure 4(a) are broader than those of the spectrum in figure 4(b), which implies that the crystallite sizes of the precipitates synthesized with liposomes are smaller than those of the precipitates without liposomes. The d -spacings obtained from the XRD pattern of the precipitates synthesized with and without liposomes compared to those from the standard x-ray data card of HAP are shown in table 1. It is clear that the precipitates synthesized both with and without liposomes perfectly match with the hexagonal phase of HAP. Because HAP in the hard tissues of the human body is also weakly crystallized phase [11], the HAP/liposome core-shell nanoparticles may be beneficial to biomedical implants.

FT-IR spectra of the precipitates are presented in figure 5. It is clear that the precipitates synthesized with liposomes have the same peaks as those without liposomes. The characteristic peaks in HAP, corresponding to the stretching vibration of PO_4^{3-} (961.0, 1037.1 and 1097.0 cm^{-1}) and deformation vibrations of PO_4^{3-} (565.1 and 602.8 cm^{-1}), appear in the two spectra. Peaks of H–O–H (1636.7, 2852.8, 2924.4, and 3417.0 cm^{-1}) and CO_3^{2-} (875.0 and 1420.7 cm^{-1}) are also observed in both systems. The bands at 3570 and 633 cm^{-1}

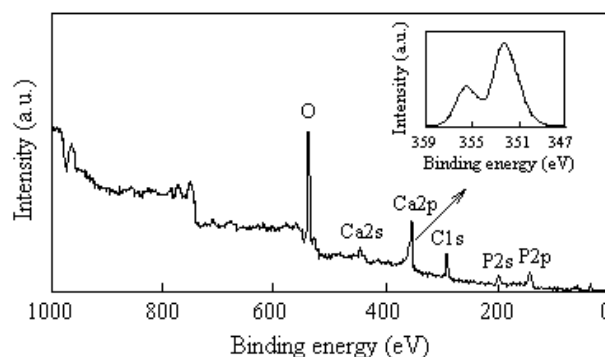


Figure 6. XPS wide scan of the surface of the precipitate powders separated from liposomes.

derived from stretching and vibrational modes of hydroxyl in HAP [12] are nearly invisible in the spectra, which further implies that the HAP synthesized both with and without liposomes is quite weakly crystallized.

In order to determine the elements at the surface of the precipitates separated from liposomes, an XPS wide scan was employed (figure 6). It can be seen that the surface of the precipitate powders has elements of Ca and P, which are the primarily chemical composites in HAP. The presence of C and O comes mainly from atmosphere when the sample is briefly exposed to air. We observe that the spectrum of Ca 2p has two peaks separated by about 3.5 eV in binding energy. The molar ratio of Ca to P at the surface of the precipitates is approximately 1.66, corresponding to 62.4% Ca and 37.6% P, which is calculated by dividing the area of the XPS lines by their respective sensitivity factors ($S_{\text{Ca}} = 0.71$, $S_{\text{P}} = 0.25$).

4. Conclusions

In summary, single-compartment unilamellar vesicles of liposomes have been used as microreactors for preparation of HAP nanoparticles. The obtained nanocomposites displayed core-shell characteristics, and the HAP cores were well protected by lipid membrane. The precipitates grown within liposomes were composed of many nanoscale rod-like whiskers with poorly crystallized apatite structure. The crystal growth was controlled by liposomes, and the sizes of whiskers were significantly reduced compared to those of whiskers grown in the absence of liposomes. Further investigation of the bioactivity and biocompatibility of the HAP/liposome core-shell nanocomposites compared to the bare HAP is being performed.

Acknowledgments

The authors would like to gratefully acknowledged Mr Thomas Glinsner, from EVG Group, Austria, for critically reading the manuscript.

References

- [1] Glimcher M J 1984 *Phil. Trans. R. Soc. B* **304** 479
- [2] Damien C J and Parsons J R 1990 *J. Appl. Biomater.* **2** 187

- [3] Huang J, Liu K, Cheng C, Ho K, Wu Y, Wang C, Cheng Y, Ko W and Liu C 1997 *Kaohsiung J. Med. Sci.* **13** 213
- [4] Feng L, Yan Y, Chen W and Li S 1998 *Chin. J. Biomed. Eng.* **17** 374
- [5] Xia Q, Chen D, Lin H, Yan Y, Feng L and Li S 1999 *J. Wuhan Univ. Tech.* **21** 5
- [6] Li S, Zhang S, Chen W and Wen O 1996 *Bioceramics* **9** 225
- [7] Bourger K N J, Staffhorst R W H M, de Vijlder H C, Velinova M J, Bomans P H, Frederik P M and de Kruijff B 2002 *Nat. Med.* **8** 81
- [8] Feng Q, Chen Q, Wang H and Cui F 1998 *J. Cryst. Growth* **186** 245
- [9] Grit M, Underberg W J M and Crommelin D J A 1993 *J. Pharm. Sci.* **82** 362
- [10] Weng G, Cheng M and Wang L 1990 *Prog. Biochem. Biophys.* **17** 76
- [11] Ohmae H, Okazaki M and Hino T 1989 *Bioceramics* vol 1, ed H Onnishi, H Aoki and K Sawai (Tokyo: Ishiyaku Euro Asmerica Inc. Press) p 80
- [12] Shirkhazadeh M 1995 *J. Mater. Sci. Mater. Med.* **6** 90